A robust optimisation model and cutting planes for the planning of energy-efficient wireless networks ☆

Grit Claßen [a,b,*], Arie M.C.A. Koster [a], Anke Schmeink [b]

[a] Lehrstuhl II für Mathematik, RWTH Aachen University, 52056 Aachen, Germany
[b] UMIC Research Centre, RWTH Aachen University, 52056 Aachen, Germany

ARTICLE INFO

ABSTRACT

In this paper, we present an optimisation model for the energy-efficient planning of future wireless networks. By applying robust optimisation, we extend this model to a robust formulation which considers demand uncertainties. The computability of the resulting model is moderate. Hence, we apply three different cutting plane approaches for an improvement. Furthermore, an extensive case study is performed to examine the price of robustness, to compare the robust solution to conventional planning, and to explore the performance of the cutting planes.

1. Introduction

Wireless networks consume an increasing amount of energy. As an example, the energy consumption of Vodafone Group increased by about 35% from 2008/09 to 2010/11 [28]. Such an increase is mainly caused by drastically rising user demands which lead to the necessity of installing more base stations (BSs) implying a higher energy consumption (not only by signal power but also by air-conditioning, etc. [11]). Thus, in 2010/2011 Vodafone Group operated 224,000 BSs with a total energy consumption of 4117 GWh [28]. These high user demands nowadays (compared to the requirements for ordinary telephony and short message services) result from, e.g., traffic-intensive smartphone applications and will continue to rise due to novel applications such as Car-to-X communication, augmented reality or Ambient Assisted Living.

User demands and resource restrictions have been considered in the planning of third generation (3G) networks [1,12,15,25]. Nevertheless, these networks reach the limits of their capacity, which means that high data rates can be offered, but only for some users and with limited coverage. One way to tackle the problem of insufficient network performance is to utilise a couple of advanced techniques such as Orthogonal Frequency Division Multiple Access (OFDMA) for future wireless networks. However,

an optimal planning is of utmost importance to fully utilise the gains of those techniques and to reduce the energy consumption.

The energy efficiency of wireless networks has recently attracted a great deal of attention: [2,7,8,14,23,24] and references therein, to name just some publications. Current methods for the planning of energy-efficient networks require a deterministic model of the problem at hand. Many factors in the real problem are, however, non-deterministic. User movements as well as fluctuating bit rate requirements and channel conditions are just three of prominent examples of uncertain parameters.

A special sector of mathematical optimisation which allows to handle uncertain data is robust optimisation. If the probability distribution of the uncertain factors is unknown, the Γ-robustness concept introduced by Bertsimas and Sim [3,4] is a promising approach. This approach limits the number of uncertain entries by a robustness parameter Γ. The robustness of the solution can then be adapted by varying the parameter. At the same time, the complexity of the problem is not significantly increased.

In this paper, we present an integer linear program (ILP) for the planning of energy-efficient wireless networks which considers downlink (DL) data transmission and guarantees a certain link quality while inter-cell interference is limited by means of a conflict graph. The ILP is based on [13] and was first presented in [9]. To extend the deterministic model to a robust formulation, we apply the Γ-robustness approach while considering uncertain user demands. Exploiting linear programming duality, the resulting robust reformulation is again linear. The increased number of variables and constraints however make the robust formulation computationally less tractable than the deterministic model.

To increase the performance of ILP solvers, we apply three types of cutting planes (cuts) to our robust optimisation model. On the one hand, we implement the well-known variable upper bounds and maximal clique inequalities. On the other hand, we extend the class of cover inequalities, known for the knapsack

problem, to robust cover inequalities following an approach presented in [18]. The separation problem for this class of valid inequalities is solved via a heuristic approach.

In our computational study, we focus on the comparison of the robust planning model with conventional wireless network planning and on the price of robustness. Additionally, we briefly discuss an alternative single objective formulation and evaluate the performance of the different cutting plane approaches.

The remainder of this paper is organised as follows. In Section 2, we present the system model and an ILP for the planning of energy-efficient but static wireless networks. To deal with demand uncertainties, we derive a robust optimisation model in Section 3. By means of three types of cuts, which are presented in Section 4, we enhance the computability of the robust model. In Section 5, we present an extensive computational study to demonstrate the gains of our robust formulation and to evaluate the performance of the cuts. Furthermore, we discuss an alternative single objective formulation leading to pareto optimal solutions. We conclude this paper with some final remarks in Section 6.

2. Preliminaries and deterministic problem formulation

In this section, we first give some preliminaries before stating an optimisation model for the energy-efficient wireless network planning problem considering DL data transmission (cf. [9]).

BS candidate sites, that is site location and configurations, are consolidated in the set S. Each BS $s \in S$ consumes power p_s and provides a total DL bandwidth b_s if it is deployed. We merge the traffic demand of users in a small area to a single traffic demand node (TN) [16,26]. The set of TNs is denoted by T. Each $t \in T$ has a demand w_t and can be assigned to at most one BS representing hard handover, which applies, e.g., to 4th generation networks.

In future wireless networks, which utilise techniques such as OFDMA, no intra-cell interference occurs and is thus left out in our model. On the other hand, we limit inter-cell interference by requiring that the installed BSs have to constitute an *independent set* in a predefined conflict graph $G = (S,E)$. An independent set is a subset $S' \subseteq S$ such that there does not exist an edge $ij \in E$ for all $i,j \in S'$.

To guarantee a certain link quality, we define a value e_{st}, called spectral efficiency, for each BS-TN pair (s,t). This parameter gives the ratio between data rate and bandwidth and incorporates, for example, the modulation and coding scheme that is supported by the associated signal-to-noise ratio (SNR). To establish a transmission link, the spectral efficiency must exceed a certain threshold $e_{\min}$. (Note that this restriction implicitly also guarantees a minimum SNR.) This constraint is included in the following auxiliary sets of indices:

$$S*T := \{(s,t) \in S \times T : e_{st} \geq e_{\min}\},$$

$$S_t := \{s \in S : (s,t) \in S*T\} \quad \forall t \in T,$$

$$T_s := \{t \in T : (s,t) \in S*T\} \quad \forall s \in S.$$

The amount of bandwidth that is allocated to TN t from BS s, if t is served by s, can be computed by division of demand w_t by spectral efficiency e_{st}.

The variables we utilise in our problem formulation are denoted as follows. Let $x_s \in \{0,1\}$ indicate whether or not BS $s \in S$ is deployed and $z_{st} \in \{0,1\}$ whether $t \in T_s$ is assigned to s. Furthermore, we introduce a slack variable u_t which is equal to one if TN t is *not* served by *any* BS. The objective is to minimise the total power consumption of the network while the number of covered TNs is maximised. Hence, the number of TNs not served by any BS is minimised. (Without this part, the optimal solution would be zero.) To combine these conflicting objectives, we

introduce a scaling parameter λ. Note that instead of using the scaling parameter λ, it is also possible to formulate a single objective model as we will discuss in Section 5.4.

The multi-objective optimisation model can now be written as

$$\min \quad \sum_{s \in S} p_s x_s + \lambda \sum_{t \in T} u_t, \tag{1a}$$

$$\text{s.t.} \quad \sum_{s \in S_t} z_{st} + u_t = 1 \quad \forall t \in T, \tag{1b}$$

$$x_i + x_j \leq 1 \quad \forall ij \in E, \tag{1c}$$

$$\sum_{t \in T_s} \frac{w_t}{e_{st}} z_{st} \leq b_s x_s \quad \forall s \in S, \tag{1d}$$

$$x_s, z_{st}, u_t \in \{0,1\} \quad \forall s \in S, \ (s,t) \in S*T, \ t \in T. \tag{1e}$$

Constraints (1b) ensure that all TNs are either covered by exactly one BS or not covered at all. Constraints (1c) guarantee an independent set of deployed BSs, whereas constraints (1d) ensure that the total bandwidth allocated does not exceed the total available DL bandwidth. For each BS s the latter constraint represents a capacity constraint, hence a *knapsack constraint* with variable right hand side. Furthermore, these constraints implicitly make sure that a TN can be assigned to a BS if and only if this BS is deployed. Model (1) has $|S| + |S*T| + |T|$ variables and $|T| + |E| + |S|$ constraints.

3. Γ-Robust formulation

Many factors of wireless networks are uncertain such as channel conditions or bit rate requirements. In this paper, we focus on the uncertainty of TN demands. These incorporate fluctuating bit rate requirements of the mobile users as well as the movement of users: If a user moves from one area, aggregated as TN t_1, to another, denoted by TN t_2, the demand value w_{t_1} will decrease while w_{t_2} will rise.

To incorporate these uncertainties in model (1), we apply the robust optimisation approach presented in [4]. The demand values are now modelled as symmetric and bounded random variables $\tilde{w}_t$ that take values in the interval $[\overline{w}_t - \hat{w}_t, \overline{w}_t + \hat{w}_t]$, where $\overline{w}_t$ denotes a nominal value and $\hat{w}_t$ its highest deviation. We assume that at most $\Gamma \in \{0, \ldots, |T|\}$ many demand values deviate from their nominal value $\overline{w}_t$ simultaneously (in the worst case towards $\overline{w}_t + \hat{w}_t$). Hence, we replace constraints (1d) by

$$\sum_{t \in T_s} \frac{\overline{w}_t}{e_{st}} z_{st} + \max_{T' \subseteq T_s, |T'| \leq \Gamma} \sum_{t \in T'} \frac{\hat{w}_t}{e_{st}} z_{st} \leq b_s x_s \quad \forall s \in S, \tag{2}$$

which are non-linear. The obvious way to linearise (2) is to compute all possible sets T'. However, this might lead to an exponential number of constraints. In [19], computations for a structurally comparable robust problem show that the exponential-sized formulation is outperformed by the following approach:

For a fixed BS s and a solution (x,z), the maximum in constraint (2) can be formulated as the following self-contained ILP:

$$\max_{T' \subseteq T_s, |T'| \leq \Gamma} \sum_{t \in T'} \frac{\hat{w}_t}{e_{st}} z_{st} = \max \quad \sum_{t \in T_s} \frac{\hat{w}_t}{e_{st}} z_{st} \varphi_t \tag{3a}$$

$$\text{s.t.} \quad \sum_{t \in T_s} \varphi_t \leq \Gamma \tag{3b}$$

$$\varphi_t \in \{0,1\} \quad \forall t \in T_s. \tag{3c}$$

Since z_{st} is fixed, the objective is not quadratic but linear. Here, φ_t is a binary variable denoting the selection of T_s. It is easy to verify that (3) is equivalent to its LP relaxation. Thus, LP duality can be

exploited and results in the dual formulation

$$\max_{T' \subseteq T_s, |T'| \le \Gamma} \sum_{t \in T} \frac{\hat{w}_t}{e_{st}} z_{st} = \min \Gamma \mu_s + \sum_{t \in T_s} v_{st} \tag{4a}$$

$$\text{s.t.} \quad \mu_s + v_{st} \ge \frac{\hat{w}_t}{e_{st}} z_{st} \quad \forall t \in T_s \tag{4b}$$

$$\mu_s \ge 0, \ v_{st} \ge 0 \quad \forall t \in T_s. \tag{4c}$$

Now, we can replace the maximum in constraints (2) by (4a) and adding constraints (4b) and (4c). Since we have a less-than-or-equal condition, we can weaken the constraint by ignoring the minimum condition, which then results in a linear formulation. The complete robust model now reads

$$\min \quad (1a)$$
$$\text{s.t.} \quad (1b), (1c), (1e)$$

$$\sum_{t \in T_s} \frac{\overline{w}_t}{e_{st}} z_{st} + \Gamma \mu_s + \sum_{t \in T_s} v_{st} \le b_s x_s \quad \forall s \in S \tag{5a}$$

$$\mu_s + v_{st} \ge \frac{\hat{w}_t}{e_{st}} z_{st} \quad \forall (s,t) \in S * T \tag{5b}$$

$$\mu_s \ge 0, \quad v_{st} \ge 0 \quad \forall s \in S, \ (s,t) \in S * T. \tag{5c}$$

Note that (5) has, compared to (1), $|S| + |S*T|$ extra variables and $|S*T|$ extra constraints.

4. Cutting planes

A standard procedure for solving ILPs is the branch-and-bound algorithm. It can significantly be improved by cutting planes, i.e., inequalities that are valid for all integer solutions but not for some solutions of the linear relaxation. By means of such inequalities, non-integer linear relaxation solutions can be cut off.

Valid inequalities such as Gomory cuts are internally generated by state-of-the-art ILP solvers like CPLEX [17]. However, ILP solvers cannot take advantage of the particular problem structure known to the user. For the problem at hand, we identified a number of problem-specific cutting planes, partly well-known for substructures contained in (5).

4.1. Variable upper bounds [27]

Constraints (1d) and therefore, also (5a) implicitly ensure that a TN can be assigned to a BS if and only if this BS is deployed. It is well-known that (5) can be strengthened by adding these constraints explicitly as

$$z_{st} \le x_s \quad \forall (s,t) \in S * T. \tag{6}$$

4.2. Maximal clique inequalities [22]

A clique is a complete subgraph. Formally speaking, let $G = (S, E)$ be a graph and $U \subseteq S$ a subset of the vertex set. We call U a clique if there exists an edge $uv \in E$ for all $u, v \in U$. A clique is maximal if it is not included in a larger clique.

Constraints (1c) describe an independent set polytope. Thus, we can replace these constraints by all maximal clique inequalities

$$\sum_{s \in U} x_s \le 1 \quad \forall U \subset S, \ U \text{ is a maximal clique in } G = (S, E). \tag{7}$$

Though NP-complete, all maximal cliques can be computed by the Bron–Kerbosch algorithm [5] without much effort.

4.3. Robust cover inequalities

Since constraints (1d) resemble a knapsack constraint for each BS s, constraints (2) are closely related to the *robust knapsack problem*. The general structure of such constraints can be written as

$$\sum_{i \in I} \overline{a}_i y_i + \max_{J \subseteq I : |J| \le \Gamma} \sum_{i \in J} \hat{a}_i y_i \le bx, \tag{8}$$

where I denotes the set of items (TNs), $\overline{a}_i$ the nominal knapsack weight, $\hat{a}_i$ its deviation, and b the knapsack capacity. For $x=1$, constraint (8) states a robust knapsack. Since $x=0$ implies $y_i=0$ for all $i \in I$, every valid inequality for the robust knapsack problem can be adapted to a valid inequality for (8) (and thus for (5)) by multiplying its right hand side with x.

One type of cuts for the knapsack problem are the well-known *cover inequalities*. They can be generalised to be applicable to the robust knapsack problem as follows (cf. [18]). A set $(C \cup J) \subseteq I$ is a *robust cover* if

$$|J| \le \Gamma, \ |C| \ge 0 \quad \text{and} \quad \sum_{i \in C} \overline{a}_i + \sum_{i \in J} (\overline{a}_i + \hat{a}_i) > b.$$

For any robust cover $C \cup J$, the *robust cover inequality* reads

$$\sum_{i \in C \cup J} y_i \le (|C \cup J| - 1) x \tag{9}$$

and is valid for (8).

Cover inequalities can be strengthened by means of the concept of *extended covers*; a first extension is presented in [18], a stronger one in [6]. To extend a robust cover $C \cup J$, we select an item $i \notin C \cup J$ whose nominal weight $\overline{a}_i$ is greater than or equal to the maximum nominal weight in C and whose peak weight $\overline{a}_i + \hat{a}_i$ is greater than or equal to the maximum peak weight in J. Together with this item, at most $|C \cup J| - 2$ items of the robust cover can be put in the knapsack at the same time. Hence,

$$\sum_{i \in E(C,J)} y_i \le (|C \cup J| - 1) x \tag{10}$$

is also valid, with $E(C,J)$ defined by

$$E(C,J) := (C \cup J) \cup \left\{ i \in I : \overline{a}_i \ge \max_{j \in C} \overline{a}_j, \ \overline{a}_i + \hat{a}_i \ge \max_{j \in J} (\overline{a}_j + \hat{a}_j) \right\}. \tag{11}$$

Separation of robust cover inequalities: Since there exist (exponentially) many robust cover inequalities, we cannot add all to (5) in advance. Instead, we separate robust cover inequalities on the fly. Given a non-integral LP solution $(\tilde{y}, \tilde{x})$, the separation problem is formulated as the following auxiliary ILP [18]:

$$\min \quad \sum_{i \in I} (\tilde{x} - \tilde{y}_i) r_i \tag{12a}$$

$$\text{s.t.} \quad \sum_{i \in I} (\overline{a}_i r_i + \hat{a}_i q_i) > b \tag{12b}$$

$$\sum_{i \in I} q_i \le \Gamma \tag{12c}$$

$$q_i \le r_i \quad \forall i \in I \tag{12d}$$

$$r_i, q_i \in \{0, 1\} \quad \forall i \in I. \tag{12e}$$

The objective (12a) minimises the reduced costs. If the optimal objective value is less than $\tilde{x}$, the robust cover $C \cup J$ defines a violated inequality of type (9) with $C := \{i \in I : r_i = 1, q_i = 0\}$ and $J := \{i \in I : q_i = 1\}$. Hence, constraint (12b) guarantees that the items in the cover violate the capacity constraint and constraint (12c) ensure that at most Γ many items can be considered with their peak demand. Finally, the peak demand can only be considered if the item is included in the cover, see constraints (12d).

The separation problem (12) is also a kind of knapsack problem, thus, NP-hard. This is why we adapt the separation heuristic given in [18] for robust cover inequalities, see Algorithm 1.

In Step 0 we sort the items according to the smallest ratios of profit (12a) to weight (12b) and initialise the parameters $\nu, \overline{V}$ and $\hat{V}$. At the end of the algorithm, ν presents the objective value of the separation problem, $\overline{V}$ the sum of the nominal weights ($\overline{a}_i$) of all items in $C \cup J$ and $\hat{V}$ presents the sum of the deviations ($\hat{a}_i$) of the items in J. Then in Step 1, those items whose peak weights are considered in the robust cover are consolidated in set J. As soon as the knapsack capacity is exceeded, the algorithm stops. Otherwise, the algorithm continues with Step 2. In this step, all resulting items with the highest nominal weights are added to the set C until the capacity is exceeded. Additionally, sets J and C are reshuffled such that J contains the items with highest deviations. When the capacity is exceeded, the algorithm stops.

After the stop of the algorithm at the end of Step 1 or Step 2, the constructed robust cover $C \cup J$ is tested for possible strengthening by removing (too) early added items and afterwards it is extended by means of (11).

Algorithm 1. Heuristic for separating robust cover inequalities

Input: weights $\overline{a}_i, \hat{a}_i$; current LP solution $\tilde{y}_i, \tilde{x}$
Output: robust cover $C \cup J$
  Step 0: Set $\nu = 0, \overline{V} = 0, \hat{V} = 0, C = \emptyset, J = \emptyset$.
    For all $i \in I$, let $\alpha_i = (\tilde{x} - \tilde{y}_i)/(\overline{a}_i + \hat{a}_i)$ and
    $\beta_i = (\tilde{x} - \tilde{y}_i)/\overline{a}_i$.
  Step1: Let $L(k)$ be the index of the kth smallest coefficient
    in $\{\alpha_i\}_{i \in I}$.
    for $k = 1$ to Γ **do**
      $J \leftarrow J \cup \{L(k)\}$
      $\overline{V} \leftarrow \overline{V} + \overline{a}_{L(k)}$
      $\hat{V} \leftarrow \hat{V} + \hat{a}_{L(k)}$
      $\nu \leftarrow \nu + (\tilde{x} - \tilde{y}_{L(k)})$
      if $\overline{V} + \hat{V} > b$ and $\nu < \tilde{x}$ **then**
        STOP
      end if
    end for
  Step 2: Let $L'(k)$ be the index of the kth smallest coefficient
    in $\{\beta_i\}_{i \in I \setminus J}$.
    for $k = 1$ to $|I| - \Gamma$ **do**
      $\overline{V} \leftarrow \overline{V} + \overline{a}_{L'(k)}$
      if $\hat{a}_{L'(k)} > \min_{i \in J} \hat{a}_i$ **then**
        $j := \underset{i \in J}{\operatorname{argmin}} \hat{a}_i$
        $C \leftarrow C \cup \{j\}$
        $J \leftarrow J \setminus \{j\} \cup \{L'(k)\}$
        $\hat{V} \leftarrow \hat{V} - \hat{a}_j + \hat{a}_{L'(k)}$
      else
        $C \leftarrow C \cup \{L'(k)\}$
      end if
      $\nu \leftarrow \nu + (\tilde{x} - \tilde{y}_{L'(k)})$
      if $\overline{V} + \hat{V} > b$ and $\nu < \tilde{x}$ **then**
        STOP
      end if
    end for

5. Computational study

In this section, we describe a computational study to reveal the added value of the robust optimisation approach. We start with a description of the considered scenarios followed by a discussion of the performance of the proposed cuts. Afterwards, we analyse the robust results regarding an alternative single objective formulation for computing pareto optimal solutions. Finally, we evaluate the robust solutions such that we can determine a good choice for Γ and we compare the corresponding network designs with conventional solutions.

5.1. The scenarios

The proposed model is tested for planning scenarios based on signal propagation data for Munich, available at [10]. We construct 21 different planning scenarios based on this data set, which comprises 60 BS candidate sites. For all scenarios, we randomly choose BSs from the 60 available and consider randomly distributed TNs. Due to this randomness it is possible that the solving performance of the created scenarios varies. To demonstrate that these variations are limited, we create ten scenarios with 40 randomly chosen BSs and 450 randomly distributed TNs (denoted by s450_40a to s450_40j). To examine the behaviour of our model for different numbers of BSs and TNs, we vary these numbers creating 11 scenarios as depicted in Table 1.

Signal prediction, which is needed for the computation of the spectral efficiencies, is done by a cube oriented ray launching algorithm [20]. Furthermore, two BSs are adjacent in the conflict graph if and only if the distance between them is less than or equal to 500 m. The resulting graph is exemplarily illustrated for scenario s450_40a in Fig. 1.

For all 21 scenarios, we use the following parameters: $b_s = 10$ MHz, $p_s = 4000$ W $\forall s \in S$ (based on [11]) and $e_{\min} = 0.5$ bps/Hz.

Since user data is not available due to data privacy limitations, we compute the demand values $\overline{w}_t$ and $\hat{w}_t$ for each $t \in T$ by

Table 1
Considered scenarios.

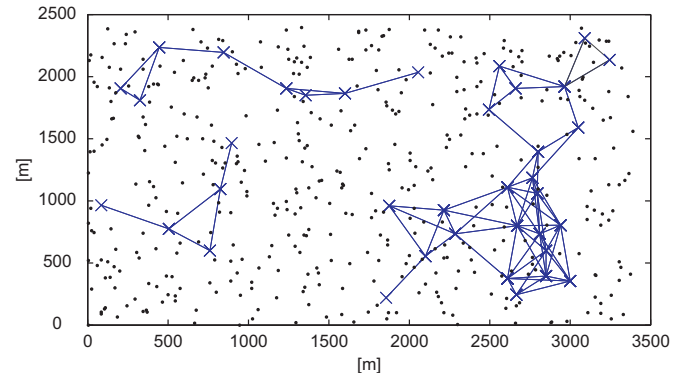| Name	Number of BSs	Number of TNs
s450_40a to s450_40j	40	450
s450_50	50	450
s450_60	60	450
s500_40	40	500
s500_50	50	500
s500_60	60	500
s550_40	40	550
s550_50	50	550
s550_60	60	550
s600_40	40	600
s600_50	50	600
s600_60	60	600

Fig. 1. BSs (denoted by blue crosses), TNs (denoted by black dots) and the conflict graph for scenario s450_40a. (For interpretation of the references to color in this figure caption, the reader is referred to the web version of this article.)

Table 2
Profiles for TNs.

Service	Regular (%)	High (%)	Bit rate (kbps)
Data	[10,20]	[30,40]	[512,2000]
Web	[20,40]	[40,50]	[128,512]

randomly generating user profiles from Table 2. We consider a regular traffic demand scenario for the nominal demands $\overline{w}_t$. Hence, a percentage for both data and web services is uniformly drawn from the "regular [%]" column and multiplied by a bit rate, uniformly drawn from the "bit rate [kbps]" column. The percentages for the peak demands $\hat{w}_t$ are drawn from the "high [%]" column and multiplied by another uniformly drawn bit rate. In both cases, the remaining percentage is used for Voice-over-IP (VoIP) with a bit rate of 64 kbps. We set $\overline{w}_t$ to the minimum of the two computed values and $\hat{w}_t$ is set to the absolute value of the difference of these two values. Thus, the minimum value for $\overline{w}_t$ is

$$10\% \cdot 512\,\text{kbps} + 20\% \cdot 128\,\text{kbps} + 70\% \cdot 64\,\text{kbps} = 121.6\,\text{kbps},$$

whereas the maximum of $\hat{w}_t$ is

$$40\% \cdot 2000\,\text{kbps} + 50\% \cdot 512\,\text{kbps} + 10\% \cdot 64\,\text{kbps}$$
$$- 121.6\,\text{kbps} = 940.8\,\text{kbps}.$$

The solutions of optimisation model (5) depend on the choice of the scaling parameter λ in the objective function. Therefore, we run tests for the following three values.

(i) $\lambda = 1000$, i.e., four TNs can be lost before it becomes beneficial to deploy an additional BS,

(ii) $\lambda = 2000$, i.e., if two TNs cannot be covered, it is more reasonable to deploy an additional BS, and

(iii) $\lambda = 4000$, i.e., losing one TN costs as much as deploying an additional BS.

Note that the judgements of the weighting of the values for λ are based on the value of the parameter p_s. Hence, the choice for the values of λ seems to be rather arbitrary. This is why we discuss an alternative formulation which gives the pareto optimal solutions in Section 5.4.

All computations are performed with CPLEX 12.2 [17] on a Linux machine with 2.93 GHz Intel Xeon X5570 processor, a memory limit of 11 GB RAM and a general CPU time limit of 1 h. To obtain comparable results with/without the separation of cutting planes, the number of used threads is fixed to one.

We compute the solutions for different Γ in decreasing order. Since the primal bound of the problem with $\Gamma = n+1$ is also an upper bound for the problem with $\Gamma = n$, we use the primal solutions found in the subsequent computations.

5.2. Cutting plane analysis

In all subsequent computations, we apply the cutting plane approaches presented in Section 4. Therefore, we investigate the performance of the cuts before evaluating our robust optimisation model.

To analyse the cuts, we run tests in the root node since, e.g., the separation of robust cover inequalities is only performed in the root node. We compute the additional gap closed which is given by

$$\frac{DB_{cut} - DB_{root}}{PB_{best} - DB_{root}},$$

where PB_{best} is the best known solution, DB_{root} the dual bound computed in the root node without the application of any type of

cut (also no internal cuts of CPLEX) and DB_{cut} is the dual bound found in the root node when the studied cuts are applied. In the case that $PB_{best} - DB_{root} = 0$, the additional gap closed is set to 0%. So the additional gap closed gives the percentage of gap between the best known solution and the current dual bound that could be closed when applying the cuts. Note that in the case we do not separate inequalities, we only solve the LP relaxation of model (5), if necessary adapted by (6) and/or (7). The optimal solution is then denoted by DB_{root} or DB_{cut}, respectively, since the optimal LP solution is comparable with the dual bound found in the root node of the ILP formulation.

We examined the variable upper bounds (6), the maximal clique inequalities (7) and the separation of robust extended cover inequalities (11) separately as well as in different combinations. Fig. 2(a) displays the additional gap closed achieved by the application of the variable upper bounds for the different values of Γ and λ. The displayed values are averaged over the scenarios s450_40a to s450_40j. We can close the optimality gap by up to 96% ($\Gamma = 0$, $\lambda = 1000$). For lower values of Γ, the closure of the gap is higher than for $\Gamma \geq 14$. However, when Γ exceeds 25, the gap closed increases again. For small and high values of Γ, the problems are easier to solve than for a medium large value. This fact will be further substantiated by the higher optimality gap (on average) in Fig. 4 for medium large Γ s, see Section 5.3.

When applying only the maximal clique inequalities, we experienced that this type of cutting plane on its own does not support the solver in closing the optimality gap significantly. The maximum
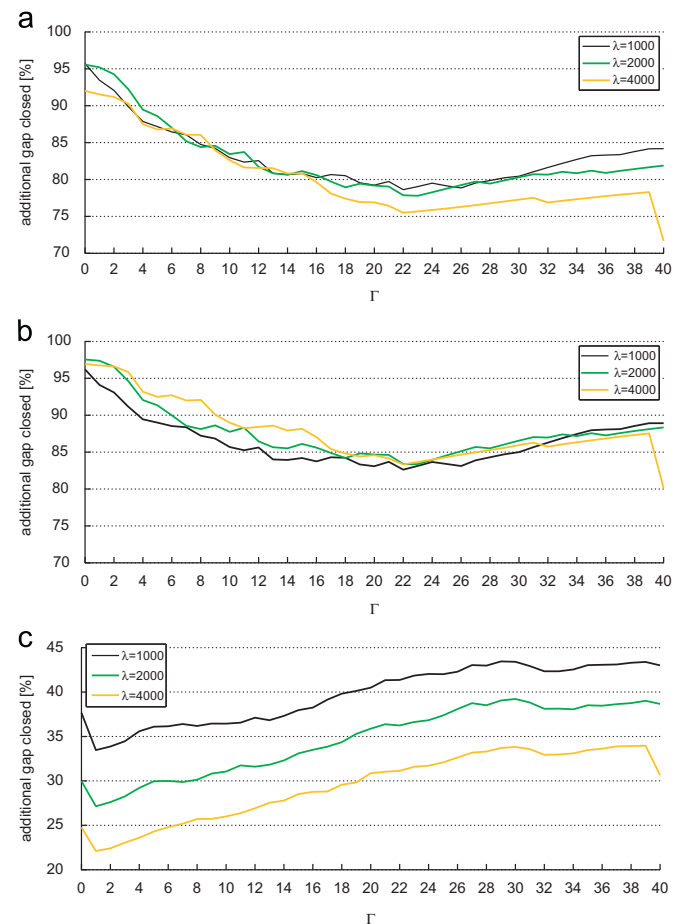
Fig. 2. Additional gap closed for the different types of cutting planes, averaged over scenarios s450_40a to s450_40j. (a) Variable upper bounds. (b) Variable upper bounds and maximal clique inequalities. (c) Separation of extended robust cover inequalities. Note, different scale!
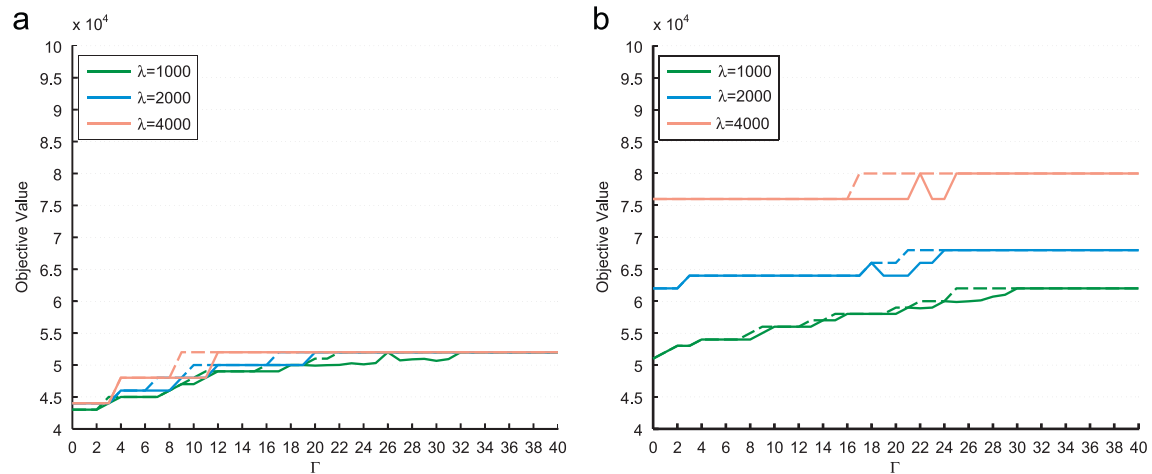
Fig. 3. Primal (dashed lines) and dual bounds (solid lines) for $\lambda \in \{1000, 2000, 4000\}$ and $\Gamma \in \{0, 1, \ldots, 40\}$. (a) s450_40a. (b) s450_40f.

additional gap closed (averaged over the scenarios s450_40a to s450_40j) is 1.28%. Nevertheless, applying variable upper bounds and maximal clique inequalities simultaneously, the gap can be closed by up to 98% ($\Gamma = 0$, $\lambda = 2000$), see Fig. 2(b). In all cases, the gap could be closed more than by applying only the variable upper bounds (ranging from 0.5% to 9.23% more). Due to this synergy effect, also the maximal clique inequalities are a reasonable approach to improve the computability of the robust model (5).

The gap closed, averaged over scenarios s450_40a to s450_40j, for the separation of robust extended cover inequalities only is presented in Fig. 2(c). For this type of cutting planes, the gap could be closed by up to 43%. The courses of the curves are (almost) the same for different values of λ. This is the case since the robust cover inequalities push the number of unsigned TNs and together with the fact that the multi-objective parameter λ behaves as a scaling parameter for the root node computations when applying the separation procedure. Only when applying all three types of cutting planes, the gap could incidently be closed by 100% ($\Gamma = 0$, $\lambda = 2000$).

Since the presented cuts can significantly improve the solving performance of the robust optimisation model (5), from now on we apply the cuts in all computations.

5.3. The price of robustness

In this subsection, we analyse the solutions (primal and dual bounds and the optimality gap) of the robust model (5) for the scenarios described in Section 5.1, and for different values of Γ and λ.

For two selected scenarios of s450_40a to s450_40j (s450_40a and s450_40f), Fig. 3 shows for $\Gamma \in \{0, 1, \ldots, 40\}$ and $\lambda \in \{1000, 2000, 4000\}$ the best solution found (primal bound) and a lower bound on the optimal solution value (dual bound), while for scenarios s450_50 to s600_60, Fig. 5 depicts these values only for selected values of Γ, $\Gamma \in \{0, 5, 10, 15, 20, 25, 30, 35, 40\}$. The plots for the remaining scenarios can be found in the Appendix, see Fig. A1.

In about 75% of the cases for scenarios s450_40a to s450_40j both bounds match, which means that the optimal solution is found within the given time limit. We observe that the objective values increase with increasing Γ (the course of the bounds is similar, independent of λ). This increase is the so-called *price of robustness*, i.e., for larger values of Γ, the solution becomes more conservative and at the same time more robust against deviations. Also the optimality gap increases with increasing Γ, but for half of the scenarios (s450_40a, s450_40b, s450_40c, s450_40f, s450_40g) only until Γ becomes too large (say 25–30). If Γ
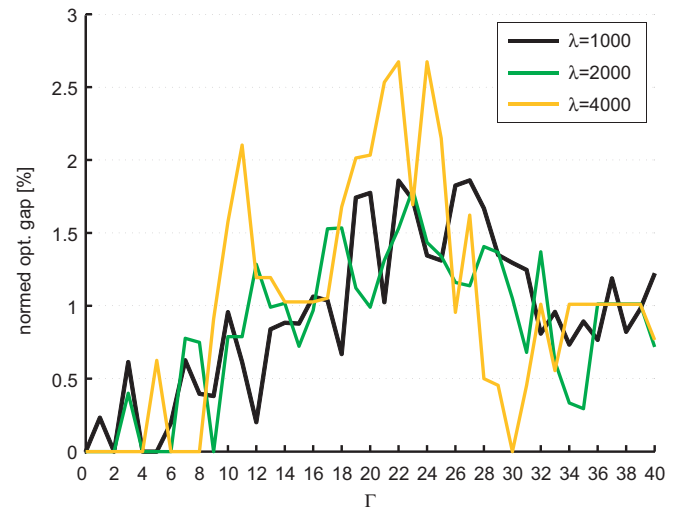

Fig. 4. Normed optimality gap averaged over scenarios s450_40a to s450_40j.

exceeds the maximum number of served TNs per BS in a scenario, then the problem is easier to solve than an instance with a lower Γ since all TNs can be considered at their peak demand. Thus, it happens quite regularly that the instances at the lowest and largest values for Γ are solved to optimality whereas the instances with Γ in between show optimality gaps. To demonstrate this more clearly, we take the smallest primal bound per scenario per λ as a basis and norm all other primal and dual bounds to this value. Subtracting the normed dual bound from the normed primal bound gives the normed optimality gap which is then averaged over the scenarios, see Fig. 4. Since the behaviour of the curves in this figure is similar to the optimality gaps that can be seen in Figs. 5 and A1, the scenarios s450_40a to s450_40j are comparable and we can arbitrarily choose one (except s450_40a, see below) for the comparison with varying numbers of BSs and TNs.

As just indicated, scenario s450_40a is a special case compared to the other scenarios. For s450_40a, all 450 TNs can be covered by the installed BSs while this is not possible in the other scenarios due to the random positioning of TNs. Hence, the multi-objective parameter λ does not influence the objective value and the bounds for all values of λ coincide (see Fig. 3(a)).

The solution bounds behave as stepwise functions for all scenarios. This is the case, since Γ can be increased to a certain
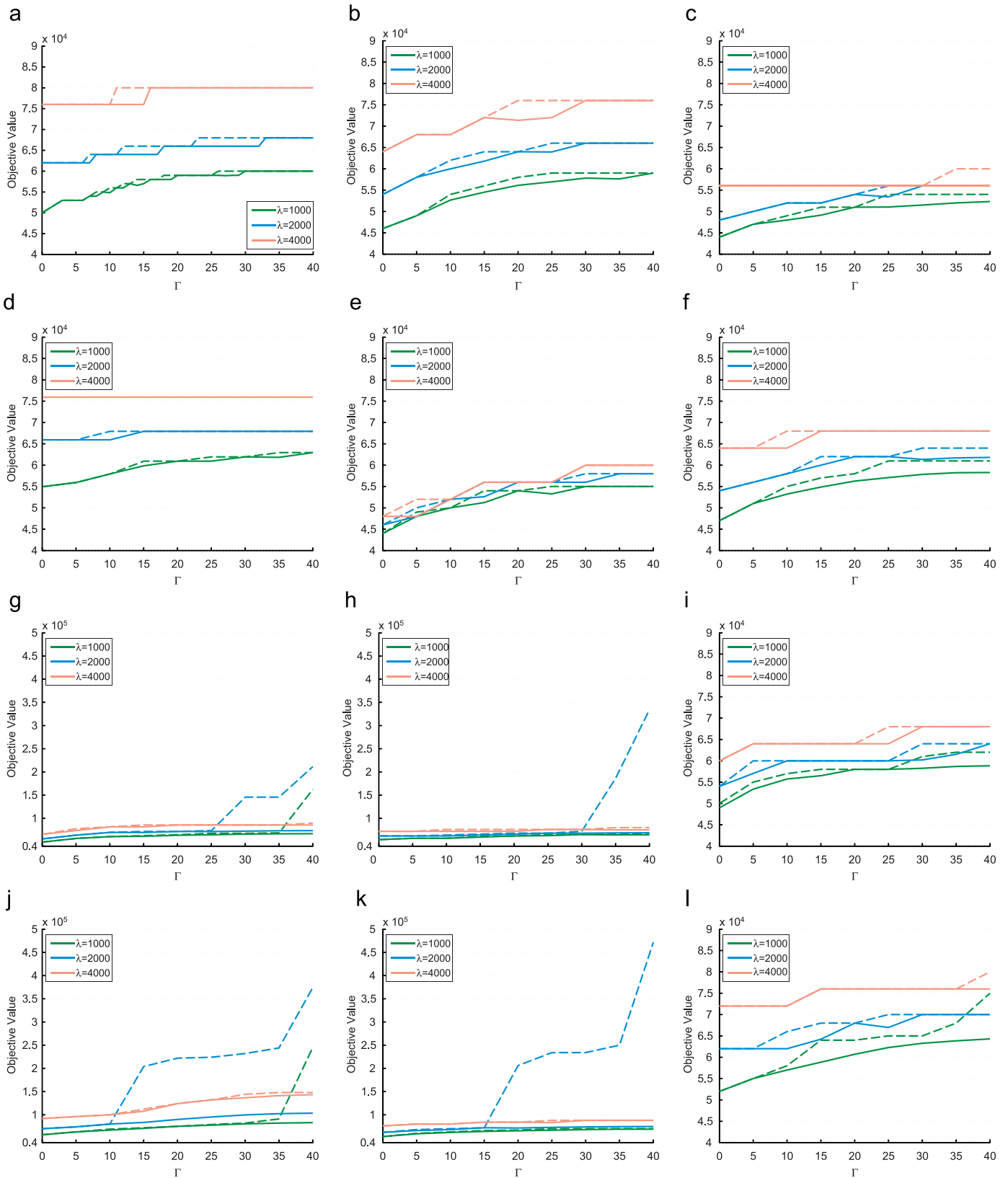
Fig. 5. Primal (dashed lines) and dual bounds (solid lines) for $\lambda \in \{1000, 2000, 4000\}$ and $\Gamma \in \{0, 5, 10, 15, 20, 25, 30, 35, 40\}$. (a) s450_40g, representative. (b). s450_50. (c) s450_60. (d) s500_40. (e) s500_50. (f) s500_60. (g) s550_40. (h) s550_50. (i) s550_60. (j) s600_40. (k) s600_50. (l) s600_60.

value, without changing the optimal solution, until the BSs cannot serve all TNs anymore. Hence, more TNs are not covered anymore and/or one more BS has to be deployed.

For the scenarios with increasing numbers of TNs and BSs (s450_50 to s600_60), about 58% of the cases could be solved to optimality within the given time limit. This number is lower than for

Fig. 6. Pareto optimal number of deployed BSs and not covered TNs for scenario s450_40g and $\Gamma = \{0, 5, 10, 20, 40\}$. (a) All pareto optimal solutions. (b) Detail of pareto optimal solutions.

scenarios s450_40a to s450_40j since a lower number of considered values for Γ also decreases the number of possible primal bounds that could be used in a solution. Obviously, scenarios with a higher number of TNs (s550_40, s550_50, s600_40 and s600_50) are more difficult to solve. Additionally, scenarios s550_60 (Fig. 5(i)) and s600_60 (Fig. 5(l)) perform better than s550_40 (Fig. 5(g)) and s600_40 (Fig. 5(j)) since it becomes easier to assign the same number of TNs to a higher number of BS candidates. However, a higher number of BSs does not necessarily improve the computability of the scenario since more BSs candidates imply a higher number of placement and assignment possibilities; the results for, e.g., s450_50 and s450_60 (Fig. 5(b) and (c)) are comparable.

5.4. Pareto optimal solutions

The computational results presented in the previous sections depend on the choice of the scaling parameter λ in the objective function. To avoid this dependency, we propose the following alternative robust formulation:

$$\min \quad \sum_{t \in T} u_t \tag{13a}$$

$$\text{s.t.} \quad \sum_{s \in S} x_s = K \tag{13b}$$

$$\text{(1b), (1c), (1e)}$$
$$\text{(5a), (5b), (5c).}$$

This model minimises the number of not covered TNs for a fixed number of deployed BSs. The number of deployed BSs is set to K, see constraint (13b). The parameter K can range between zero and the independent set number of the conflict graph, which is the maximum number of BSs that can be installed without being in conflict with each other.

By means of this model, we can compute the pareto optimal solutions for different values of the robustness parameter Γ. Pareto optimal in our context denotes the fact that we cannot deploy fewer BSs and at the same time serve the same number of TNs.

We solve formulation (13) exemplarily for scenario s450_40g with $K \in \{0, 1, \dots, 17\}$ and $\Gamma \in \{0, 5, 10, 20, 40\}$. The results are presented in Fig. 6. The independent set number of the conflict graph of scenario s450_40g is 17, i.e., $K \le 17$. Fig. 6(a) displays for every number of installed BSs how many TNs cannot be covered by the

Table 3
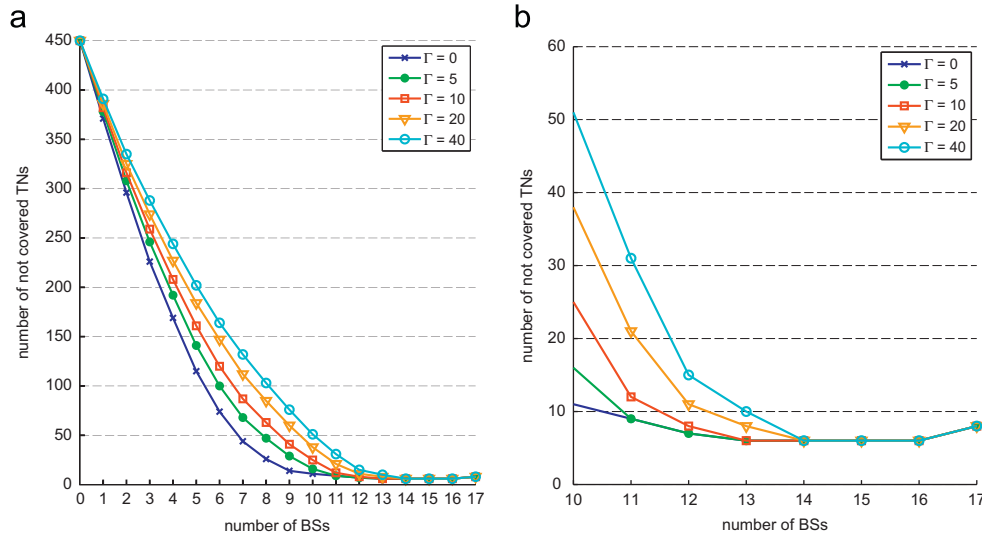Numbers of installed BSs and not covered TNs for $\lambda \in \{1000, 2000, 4000\}$ and $\Gamma \in \{0, 5, 10, 20, 40\}$.

Γ	$\lambda = 1000$		$\lambda = 2000$		$\lambda = 4000$	
	#BSs	#TNs	#BSs	#TNs	#BSs	#TNs
0	9	14	11	9	13	6
5	11	9	11	9	13	6
10	12	8	13	6	13	6
20	13	7*	13	7*	14	6
40	13	8*	14	6	14	6

best solution found after one hour of CPU time (83% of the problems are solved to optimality). Obviously, if we do not install any BS no TN can be served and hence, the curves for each Γ start at 450. However, already for $K=1$, the numbers of not covered TNs vary for different values of Γ. The larger the value of Γ, the fewer TNs can be covered by the same number of BSs. The most significant values for K are between 11 and 14, depicted in detail in Fig. 6(b). Starting from 11, the curves begin to merge such that all curves are identical for $K \ge 14$. Therefore, the highest reasonable value for K is 14.

For $K=17$, eight TNs cannot be covered whereas for $K=16$ this number is only 6. Hence, the solutions for $K=17$ are not pareto optimal. This is the case since constraint (13b) is an equality constraint. If the equality was replaced by a less than or equal sign, the objective value for K would also be 6.

The corresponding solutions of model (5) are given in Table 3. All numbers of not covered TNs, apart from the three numbers marked by ∗, lie on the corresponding curves in Fig. 6(a). For the three cases marked by ∗, either model (13) or model (5) could not be solved to optimality within 1h time limit. The numbers in Table 3 hence show that all results for the two problem formulations are comparable and it is reasonable to consider the multi-objective formulation.

5.5. Evaluation of robust planning

In Section 5.3, we have computed the solutions of the robust formulation (5) for $\Gamma \in \{0, 1, \dots, 40\}$ in the cases of scenarios s450_40a to s450_40j. In this section, we evaluate these solutions to determine a good choice for Γ (per scenario) for which the solution of the robust formulation gives a reasonable network planning, where

reasonable means being robust but not too conservative. Our evaluation is based on the probability bounds given in [4]. The probability that the capacity constraint (1d) for $s \in S$ is violated can be bounded as follows if the demand values are modelled as independent and symmetrically distributed random variables $\tilde{w}_t$ in $[\overline{w}_t - \hat{w}_t, \overline{w}_t + \hat{w}_t]$.

$$\mathcal{P}\left(\sum_{t \in T_s} \frac{\tilde{w}_t}{e_{st}} z_{st} > b_s x_s\right) \leq B(n_s, \Gamma),\tag{14}$$

where

$$B(n_s, \Gamma) = \frac{1}{2^{n_s}}\left[(1 - p_s + \lfloor p_s \rfloor)\binom{n_s}{\lfloor p_s \rfloor} + \sum_{l = \lfloor p_s \rfloor + 1}^{n_s}\binom{n_s}{l}\right],$$

with $n_s = |T_s|$ and $p_s = (\Gamma + n_s)/2$. In theory, this is the best bound possible [4]. We compute the values $B(n_s, \Gamma)$ for each BS and Γ. We study two cases: the probability $B(n_s, \Gamma)$ should either be lower than $\mathcal{P} = 5\%$ or lower than $\mathcal{P} = 1\%$. This value is to be determined by the network operator based on the fact that the lower the value for $\mathcal{P}$, the better the network is secured against bad performance due to demand fluctuations. Table 4 gives the minimum values, the values averaged over the BSs and the maximum values of Γ for which the probability $B(n_s, \Gamma)$ is lower than 5% or 1%, respectively.

In Table 4, we see that Γ has to be at least 6 (7) and at most 19 (26) if the capacity constraints (1d) should be fulfilled with probability 95% (99%). The differences in Γ for scenarios s450_40a to s450_40j are not severe. If Γ is set to the highest value, the solution will be too conservative for most BSs and if the lowest value is chosen, it will most likely happen that quite a number of capacity constraints (1d) are not fulfilled with the required probability. Thus, for the comparison of a robust solution to conventional wireless network planning in the next subsection, we set Γ to the averaged values.

5.6. Conventional wireless network planning

In this section, we compare the number of installed BSs and the number of covered TNs in a robust solution and in the solution of the conventional problem. The exact numbers of installed BSs and covered TNs can be found in the Appendix in Table A1.

For the robust solution, we consider the robust problem defined by the values of Γ given in the columns denoted by "avg" in Table 4 since for these values the capacity constraints (1d) are on average fulfilled with probability 95% and 99%, respectively. Thus, these values represent a reasonable choice for Γ.

By conventional wireless network planning we denote the planning method, in which any uncertainties of parameters are ignored; parameters are assumed to be static. However, to be able to compensate, e.g., demand fluctuations, a network operator should plan with values equal or close to the peak demand values [21]. Thus, we run model (1) with $w_t = \overline{w}_t + \hat{w}_t$ for all $t \in T$ for the

Table 4
Reasonable choices for Γ for different probability bounds.

Scenario	$\mathcal{P} = 5\%$			$\mathcal{P} = 1\%$		
	min	avg	max	min	avg	max
s450_40a	8	14	18	11	20	24
s450_40b	6	13	17	8	19	23
s450_40c	7	14	19	10	20	26
s450_40d	8	14	18	10	20	25
s450_40e	7	13	18	9	19	25
s450_40f	6	13	17	7	19	24
s450_40g	6	14	18	7	20	25
s450_40h	6	13	18	7	19	24
s450_40i	8	14	19	10	20	26
s450_40j	7	14	19	9	19	26

Table 5
Best robust solutions compared to conventional solutions for $\mathcal{P} = 5\%$.

Scenario	Best Γ	$\lambda = 1000$		$\lambda = 2000$		$\lambda = 4000$	
		ΔBSs	ΔTNs	ΔBSs	ΔTNs	ΔBSs	ΔTNs
s450_40a	14	1	−1	1	−1	0	0
s450_40b	13	1	−1	0	2	0	2
s450_40c	14	1	0	1	0	1	0
s450_40d	14	1	0	1	0	1	0
s450_40e	13	1	−1	1	−1	0	1
s450_40f	13	2	−3	1	0	1	0
s450_40g	14	1	−2	1	−1	0	0
s450_40h	13	2	−3	0	1	1	0
s450_40i	14	1	0	1	0	1	0
s450_40j	14	1	−1	0	1	0	0

Table 6
Best robust solutions compared to conventional solutions for $\mathcal{P} = 1\%$.

Scenario	Best Γ	$\lambda = 1000$		$\lambda = 2000$		$\lambda = 4000$	
		ΔBSs	ΔTNs	ΔBSs	ΔTNs	ΔBSs	ΔTNs
s450_40a	20	1	−3	0	0	0	0
s450_40b	19	1	−2	0	1	−1	1
s450_40c	20	0	1	1	−1	0	0
s450_40d	20	0	3	1	0	1	0
s450_40e	19	1	−2	0	0	0	1
s450_40f	19	1	0	1	−1	0	0
s450_40g	20	0	1	1	−1	0	0
s450_40h	19	1	−2	0	1	1	−1
s450_40i	20	1	−2	1	−1	0	0
s450_40j	19	1	−2	0	0	0	0

conventional network planning. The optimal solution is found in about 93% of the cases.

In Tables 5 and 6, we display the difference between installed BSs in the robust solution and in the conventional solution (ΔBSs) as well as the difference between the number of covered TNs in the robust solution and in the conventional solution (ΔTNs) for $\lambda \in \{1000, 2000, 4000\}$ and $\mathcal{P} \in \{5\%, 1\%\}$. A positive value in a column denoted by "ΔBSs" means that in our robust solution less BSs than in the conventional solution are deployed. Furthermore, a positive value in a column denoted by "ΔTNs" means that our robust solution can cover more TNs than the conventional solution, where a negative value means that our robust solution loses some TNs compared to the conventional solution. The robust solutions for $\mathcal{P} = 1\%$ are naturally more conservative than for $\mathcal{P} = 5\%$. Hence, for $\mathcal{P} = 5\%$ we can install up to two BSs less than in the conventional planning, where for $\mathcal{P} = 1\%$ we can install at most one BS less (saving 4000 W per fewer installed BS). The number of installed BSs ranges from 12 to 15. For both probabilities, we loose at most three TNs, which is less than 1% of the total number of TNs, but only under the circumstance that fewer BSs are deployed. The gains of the robust solutions decrease for higher values of λ. This is explained easily by the conservative choice of, e.g., $\lambda = 4000$. As stated in Section 5.1, $\lambda = 4000$ means that it becomes beneficial to deploy an additional BS if more than one TN cannot be covered. Therefore, also the robust solutions for smaller values of Γ are already quite conservative and cannot save as much energy as the solutions for smaller values of λ.

Taking the number of deployed BSs in the conventional solution as a basis, we compute the percental energy savings averaged over scenarios s450_40a to s450_40j in Table 7. Even for a quite small number of deployed BSs (at most 15), our robust solution can save up to 8.96% energy or 5.22% if the solution should be more conservative. Note that these numbers strongly depend on the multi-objective parameter λ as well as on Γ, thus on the desired choice of conservatism of the network operator. Due to the high energy savings compared to the small number of BSs, we see a high potential for

further energy savings in wireless networks of practical relevant sizes. Snapshot simulations [9] with a binary decision for each TN (considered either at the nominal or at the peak demand) have suggested comparable values of Γ ($\Gamma = 16$) for a robust planning which suffices in practice and results in similar energy savings.

6. Concluding remarks

In this paper, we have introduced a robust optimisation model for the energy-efficient planning of future wireless networks. By means of the Γ-robustness approach, we have incorporated demand uncertainties. Network operators can assess the trade-off between robustness and energy consumption, the so-called price of robustness, by varying the robustness parameter and the λ (or by pareto optimal solutions). The case study illustrated a high potential for energy savings (installing fewer BSs) by our robust solutions compared to conventional wireless network planning. Furthermore, the computational results demonstrate that the cuts, applied to enhance the computability, can actually improve the solution performance.

Acknowledgments

Appendix A

See (Fig. A1) and (Table A1)

Table 7
Percental energy savings for $\mathcal{P} \in \{1\%, 5\%\}$ averaged over scenarios s450_40a to s450_40j.

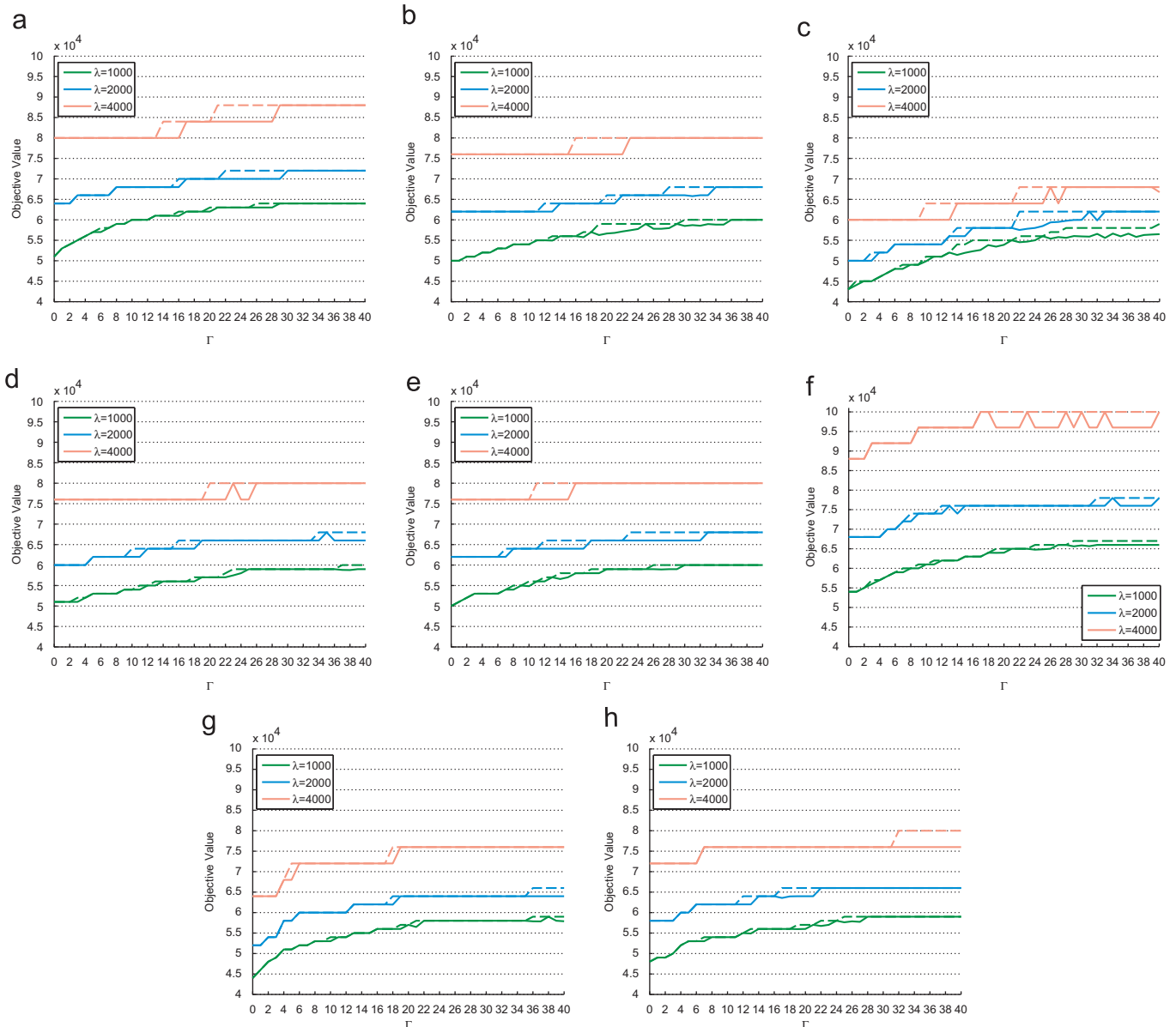| $\mathcal{P} = 5\%$			$\mathcal{P} = 1\%$		
$\lambda = 1000$	$\lambda = 2000$	$\lambda = 4000$	$\lambda = 1000$	$\lambda = 2000$	$\lambda = 4000$
8.96%	5.11%	3.52%	5.22%	3.57%	0.67%

Fig. A1. Primal (dashed lines) and dual bounds (solid lines) for $\lambda \in \{1000, 2000, 4000\}$ and $\Gamma \in \{0, 1, \ldots, 40\}$. (a) s450_40b. (b) s450_40c. (c) s450_40d. (d) s450_40e. (e) s450_40g. (f) s450_40h. (g) s450_40i. (h) s450_40j.

Table A1
Number of deployed BSs and covered TNs for the best robust solutions for $\mathcal{P} \in \{1\%, 5\%\}$ and the conventional solutions, $\lambda \in \{1000, 2000, 4000\}$.

Scenario	$\lambda = 1000$						$\lambda = 2000$						$\lambda = 4000$					
	Rob., $\mathcal{P} = 5\%$		Rob., $\mathcal{P} = 1\%$		Convent.		Rob., $\mathcal{P} = 5\%$		Rob., $\mathcal{P} = 1\%$		Convent.		Rob., $\mathcal{P} = 5\%$		Rob., $\mathcal{P} = 1\%$		Convent.	
	BSs	TNs	BSs	TNs	BSs	TNs	BSs	TNs	BSs	TNs	BSs	TNs	BSs	TNs	BSs	TNs	BSs	TNs
s450_40a	12	449	12	447	13	450	12	449	13	450	13	450	13	450	13	450	13	450
s450_40b	13	441	13	440	14	442	14	444	14	443	14	442	14	444	15	443	14	442
s450_40c	12	442	13	443	13	442	13	444	13	443	14	444	13	444	14	444	14	444
s450_40d	12	444	13	447	13	444	13	447	13	447	14	447	13	447	13	447	14	447
s450_40e	12	442	12	441	13	443	12	442	13	443	13	443	14	445	14	445	14	444
s450_40f	12	441	13	444	14	444	13	444	13	443	14	444	13	444	14	444	14	444
s450_40g	12	440	13	443	13	443	12	443	13	443	14	444	14	444	14	444	14	444
s450_40h	12	436	13	437	14	439	14	440	14	440	14	439	14	440	14	439	15	440
s450_40i	12	443	12	441	13	443	13	445	13	444	14	445	13	445	14	445	14	445
s450_40j	12	442	12	441	13	443	13	444	13	443	13	443	15	446	15	446	15	446

References

[1] Amaldi E, Capone A, Malucelli F. Radio planning and coverage optimization of 3G cellular networks. Wireless Networks 2008;14:435–47.

[2] Badic B, O'Farrell T, Loskot P, He J. Energy efficient radio access architectures for green radio: large versus small cell size deployment. In: IEEE 70th vehicular technology conference fall (VTC 2009-Fall); 2009. p. 1–5.

[3] Bertsimas D, Sim M. Robust discrete optimization and network flows. Mathematical Programming: Series B 2003;98:49–71.

[4] Bertsimas D, Sim M. The price of robustness. Operations Research 2004;52(1):35–53.

[5] Bron C, Kerbosch J. Algorithm 457: finding all cliques of an undirected graph. Communications of the ACM 1973;16:575–7.

[6] Büsing C. Recoverable robustness in combinatorial optimization. PhD thesis, Technische Universität Berlin; 2011.

[7] Chen T, Zhang H, Zhao Z, Chen X. Towards green wireless access networks. In: 5th international ICST conference on communications and networking in China (CHINACOM). p. 1–6.

[8] Chen Y, Zhang S, Xu S. 2010. Characterizing energy efficiency and deployment efficiency relations for green architecture design. In: IEEE international conference on communications (ICC). p. 1–5.

[9] Claßen, G, Koster AMCA, Schmeink A. Robust planning of green wireless networks. In: 2011 5th international conference on network games, control and optimization (NetGCooP), 2011.

[10] COST 231. Urban micro cell measurements and building data. ⟨http://www2.ihe.uni-karlsruhe.de/forschung/cost231/cost231.en.html⟩; 1996.

[11] Deruyck M, Vereecken W, Tanghe E, Joseph W, Pickavet M, Martens L, et al. Comparison of power consumption of mobile WiMAX, HSPA and LTE access networks. In: 9th conference on telecommunications internet and media techno economics (CTTE); 2010. p. 1–7.

[12] Eisenblätter A, Fügenschuh A, Geerdes H, Junglas D, Koch T, Martin A. Integer programming methods for UMTS radio network planning. In: Proc WiOpt04; 2004.

[13] Engels A, Reyer M, Mathar R. Profit-oriented combination of multiple objectives for planning and configuration of 4G multi-hop relay networks. In: 7th international symposium on wireless communication systems (IEEE ISWCS); 2010. p. 330–4.

[14] Fehske A, Richter F, Fettweis G. Energy efficiency improvements through micro sites in cellular mobile radio networks. In: IEEE GLOBECOM workshops; 2009. p. 1–5.

[15] Geerdes H. UMTS radio network planning: mastering cell coupling for capacity optimization. PhD thesis, Technische Universität Berlin; 2008.

[16] Glaßer C, Reith S, Vollmer H. The complexity of base station positioning in cellular networks. Discrete Applied Mathematics 2005;148(1):1–12.

[17] IBM – ILOG. CPLEX Optimization Studio 12.2. URL ⟨http://www.ilog.com/products/cplex⟩; 2011.

[18] Klopfenstein O, Nace D. Valid inequalities for a robust knapsack polyhedron—application to the robust bandwidth packing problem. In: Proceedings of the international network optimization conference (INOC); 2009.

[19] Koster AMCA, Kutschka M, Raack C. Robust network design: formulations, valid inequalities, and computations. Technical Report 11-34, Zuse Institute Berlin, URL ⟨http://opus4.kobv.de/opus4-zib/frontdoor/index/index/docId/1389⟩; 2011.

[20] Mathar R, Reyer M, Schmeink M. A cube oriented ray launching algorithm for 3D urban field strength prediction. In: IEEE ICC; 2007.

[21] Olinick E. Mathematical programming models for third generation wireless network design. In: Kennington J, Olinick E, Rajan D, editors. Wireless network design: optimization models and solution procedures. Springer; 2011.

[22] Padberg M. On the facial structure of set packing polyhedra. Mathematical Programming 1973;5:199–215.

[23] Richter F, Fehske A, Fettweis G. Energy efficiency aspects of base station deployment strategies for cellular networks. In: IEEE 70th vehicular technology conference fall (VTC 2009-Fall); 2009. p. 1–5.

[24] Richter F, Fehske AJ, Marsch P, Fettweis GP. Traffic demand and energy efficiency in heterogeneous cellular mobile radio networks. In: IEEE 71st vehicular technology conference (VTC 2010-Spring); 2010. p. 1–6.

[25] Siomina I, Varbrand P, Yuan D. An effective optimization algorithm for configuring radio base station antennas in UMTS networks. In: IEEE 64th vehicular technology conference (VTC 2006-Fall); 2006. p. 1–5.

[26] Tutschku K, Gerlich N, Tran-Gia P. An integrated approach to cellular network planning. In: Proceedings of the 7th international network planning symposium networks 96; 1996. p. 185–90.

[27] van Roy TJ. A cross decomposition algorithm for capacitated facility location. Operations Research 1986;34(1):145–63.

[28] Vodafone Group. Sustainability report 2010/11. URL ⟨http://www.vodafone.com/content/dam/vodafone/about/sustainability/reports/2010-11_vodafone_sustainability_report.pdf⟩; 2011.